

## SUPPORTING INFORMATION

### **Radical-translocation Intermediates and Hurdling of Pathway Defects in “Super-oxidized” (Mn<sup>IV</sup>/Fe<sup>IV</sup>) *Chlamydia trachomatis* Ribonucleotide Reductase**

Laura M. K. Dassama,<sup>1,#</sup> Wei Jiang,<sup>1,2,#</sup> Paul T. Varano,<sup>2</sup> Maria-Eirini Pandelia,<sup>2</sup> Denise A. Conner,<sup>2</sup> Jiajia Xie,<sup>1</sup> J. Martin Bollinger, Jr.,<sup>1,2,\*</sup> Carsten Krebs<sup>1,2,\*</sup>

*Departments of <sup>1</sup>Biochemistry and Molecular Biology and <sup>2</sup>Chemistry, The Pennsylvania State University, University Park, PA 16802*

<sup>#</sup>These authors contributed equally to this work.

**Simulation of Tyrosyl Radicals.** Simulation of the X-band EPR spectra of the radicals shown in Figure 3 was carried out by using *EasySpin* ([www.easyspin.org](http://www.easyspin.org)).<sup>1</sup> A total electronic spin ( $S_{\text{total}}$ ) of  $\frac{1}{2}$  was assumed. Hyperfine interactions with six nonequivalent nuclei, two  $C_{\beta}$  methylene protons and the four protons on the phenyl ring, were considered. The principal  $g$ -values of tyrosyl radicals have a polynomial dependence on the spin density of the C1 carbon, with the  $g_x$  component being the most sensitive one.<sup>2</sup> The  $g_y$  and  $g_z$  principal values vary less among the different radical signals studied.<sup>2</sup> For both radicals, the line widths were assumed to be isotropic and pseudo-Voigtian, with an additional anisotropic line broadening contribution being introduced for the radical in the wt  $\alpha\cdot\beta$  complex. The hyperfine coupling constants of the ring protons are quite conserved among different tyrosyl radicals.<sup>2</sup> Therefore, their values in the simulations were allowed to vary within a narrow range of 2 MHz of the reported, typical values.<sup>2</sup> The Euler angles between the  $A_x$  tensor component of the ring protons and the  $g_x$  direction were assumed to be similar to those previously reported.<sup>2</sup> Analysis of various tyrosyl radicals by ENDOR spectroscopy has revealed that the hyperfine tensors for the methylene protons are nearly axial, with the largest component being  $A_x$  ( $A_{\text{parallel}}$ ) and the other two components being nearly equal [ $A_y \approx A_z$  ( $A_{\text{perpendicular}}$ )].<sup>2</sup> The axial symmetry was an additional constraint for the determination of the hyperfine couplings of the methylene proton by simulations. Overall, the difference between the  $g_x$  values obtained for the  $\beta$ -wt $\cdot\alpha$ -wt and the  $\beta$ -Y<sub>338</sub>F $\cdot\alpha$ -wt complexes are indicative of different spin densities on the C1 carbon, whereas the different hyperfine couplings and their degree of anisotropy ( $A_{\text{parallel}}/A_{\text{perpendicular}}$ ) reflect a different dihedral angle,  $\theta$ , between the  $C_{\beta}$ -H

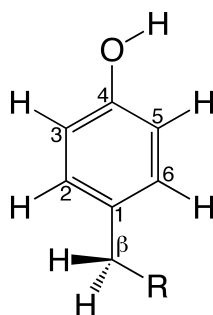
bond and the axis normal to the plane of the aromatic ring. The simulation parameters are provided in Table S1.

**Spin Quantification of EPR Signals.** The quantification of duplicate samples of *Ct*  $\beta$   $\text{Mn}^{\text{IV}}/\text{Fe}^{\text{IV}}$  and the RT pathway  $\text{Y}\cdot(\text{s})$  (see Materials and Methods for preparation of samples) were carried out as previously described.<sup>3</sup> The results are presented in **Table S2**. Samples were prepared as described in the legend of **Figure S2**.

Species	$\beta$ -wt• $\alpha$ -wt	$\beta$ -Y <sub>338</sub> F• $\alpha$ -wt
$A_{\text{H}\beta 1}$ (MHz)	31.3, 27.3, 24.0	56.0, 49.0, 49.0
$A_{\text{H}\beta 2}$ (MHz)	16.0, 15.0, 15.0	2.0, 1.0, 1.0
$A_{\text{H}3}$ (MHz) <sup>a</sup>	-24.7, -8.0, -22	-24.7, -8.0, -20.0
$A_{\text{H}5}$ (MHz) <sup>b</sup>	-26.7, -8.0, -22.4	-25.5, -8.0, -20.4
$A_{\text{H}2}$ (MHz) <sup>c</sup>	5.0, 7.5, 1.5	5.0, 7.5, 1.5
$A_{\text{H}6}$ (MHz) <sup>d</sup>	5.0, 7.5, 1.5	5.0, 7.5, 1.5
Line width (mT)	0.24, 0.25, 0.26	0.15
<b>g</b>	2.0104, 2.0045, 2.0016	2.0074, 2.0046, 2.0018

<sup>a</sup> **A** was rotated into the frame of **g** around  $A_z$  using Euler angles of  $\alpha = 22^\circ$ , <sup>b</sup>  $\alpha = -22^\circ$ , <sup>c</sup>  $\alpha = 10^\circ$ , and <sup>d</sup>  $\alpha = -10^\circ$ .

Sample	Total Area (arbitrary units)	Relative amount of $\text{Mn}^{\text{IV}}/\text{Fe}^{\text{IV}}$ (%)	Relative amount of % $\text{Y}\cdot$ (%)
- CDP, ATP (trial 1)	30	100	0
+ CDP, ATP (trial 1)	37	54	46
- CDP, ATP (trial 2)	28	100	0
+ CDP, ATP (trial 2)	29	56	44



**Scheme S1:** Schematic drawing of the phenol ring of a tyrosine residue with numerical assignments used for the simulation of the radicals.

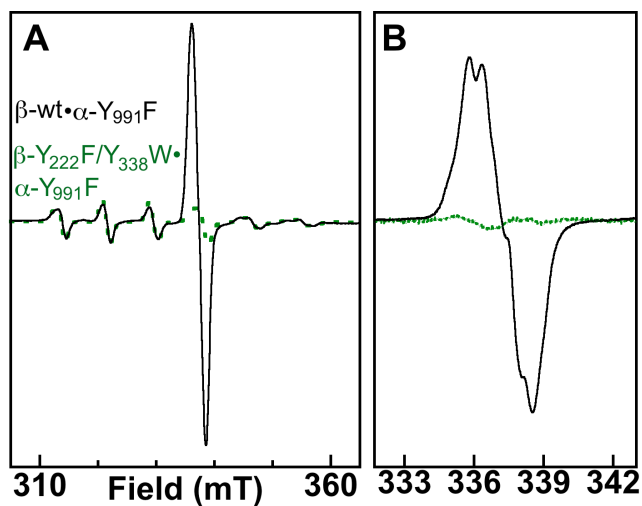


**Figure S1.** X-band EPR spectra of samples prepared with the *Ct*  $\alpha$ -Y<sub>991</sub>F variant demonstrating the generation of an organic radical when complexed with *Ct*  $\beta$ -wt (black spectra), but failure to form any significant organic radical when in complex with *Ct*  $\beta$ -Y<sub>222</sub>F/Y<sub>338</sub>W (green spectra). The “raw” spectra are shown in panel **A**, whereas spectra in panel **B** have had the contribution of the Mn<sup>IV</sup>/Fe<sup>IV</sup> states removed. Sample preparation and spectrometer conditions are identical to those described in the legend of **Figure 1**.

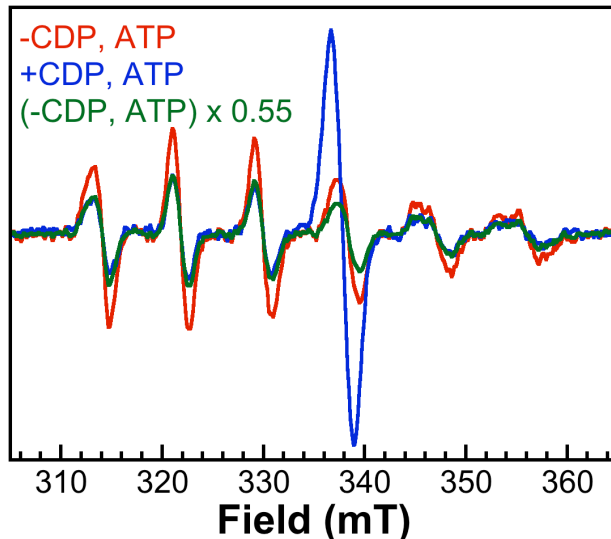


**Figure S2.** Representative X-band EPR spectra demonstrating loss of signal intensity attributable to the  $\text{Mn}^{\text{IV}}/\text{Fe}^{\text{IV}}$  intermediate upon formation of the  $\text{Y}\cdot$ .  $\text{Mn}^{\text{II}}/\text{Fe}^{\text{II}}\text{-}\beta$  was first mixed with  $\text{O}_2$ -saturated buffer to form the  $\text{Mn}^{\text{IV}}/\text{Fe}^{\text{IV}}$  intermediate, and after 2 s, the resultant solution was mixed either with  $\alpha$ ,  $\text{MgSO}_4$ , and DTT (**red spectrum**) or with one  $\alpha$ , CDP, ATP,  $\text{MgSO}_4$ , and DTT (**blue spectrum**). After mixing with the  $\alpha$ -containing solution, the reaction was quenched after 1 s by spraying the reaction mixture into cold ( $\sim 120$  K) 2-methylbutane. The intensity attributable to the  $\text{Mn}^{\text{IV}}/\text{Fe}^{\text{IV}}$  intermediate is  $\sim 45\%$  less in the spectrum of the sample in which the  $\text{Y}\cdot$  is formed than in the sample in which no  $\text{Y}\cdot$  accumulates (**green spectrum**). This loss of intensity correlates well to a  $\sim 45\%$  increase in signal intensity in the fourth line of the six packets of resonances observed. This increased intensity is attributable to the  $\text{Y}\cdot$ . Final concentrations after mixing were: 0.2 mM  $\beta$ , 0.15 mM Mn, 0.15 mM Fe, 0.3 mM  $\alpha$ , 1 mM CDP (when present), 0.5 mM ATP (when present), 10 mM  $\text{MgSO}_4$ , 10 mM DTT. The spectrometer conditions were:  $T = 14 \pm 0.2$  K, microwave frequency = 9.47 GHz, microwave power = 20  $\mu\text{W}$ , modulation

frequency = 100 KHz, modulation amplitude = 10 G, time constant = 167 ms, scan time = 167 s.

## REFERENCES

- (1) Stoll, S.; Schweiger, A. *J. Magn. Reson.* **2006**, *178*, 42-55.
- (2) Svistunenko, D. A.; Cooper, C. E. *Biophys. J.* **2004**, *87*, 582 - 595.
- (3) Dassama, L. M. K.; Yosca, T. H.; Conner, D. A.; Lee, M. H.; Blanc, B.; Streit, B. R.; Green, M. T.; DuBois, J. L.; Krebs, C.; Bollinger, J. M. *Biochemistry* **2012**, *51*, 1607-1616.